



# Spatiotemporal distribution of magmatism and crustal inheritance within an extensional–rotational environment: an updated geochronology of the Miocene and Quaternary magmatism of the South Apuseni Mountains

V. V. Ene<sup>1,2\*</sup>, S. Tapster<sup>3</sup>, D. J. Smith<sup>1</sup>, C. Panaiotu<sup>4,5</sup>, E. Roşu<sup>2</sup>, J. Naden<sup>6</sup> and M. Munteanu<sup>2</sup>

<sup>1</sup> Department of Geology, University of Leicester, University Road, Leicester LE1 7RH, UK

<sup>2</sup> Geological Institute of Romania, 1 Caransebeş Street, Sector 1, Bucharest 012271, Romania

<sup>3</sup> Geochronology and Tracers Facility, British Geological Survey, Nottingham NG12 5GG, UK

<sup>4</sup> Faculty of Physics, University of Bucharest, 077125 Măgurele, Romania

<sup>5</sup> Romanian Academy, Calea Victoriei 125, 010071 Bucharest, Romania

<sup>6</sup> British Geological Survey, Nicker Hill, Keyworth, Nottingham NG12 5GG, UK

VVE, 0009-0007-2722-8979; ST, 0000-0001-9049-0485; DJS, 0000-0002-8685-7886; CP, 0000-0001-9332-8926; JN, 0000-0003-3097-5530

\* Correspondence: [vlad-victor.ene@geodin.ro](mailto:vlad-victor.ene@geodin.ro)

Present addresses: VVE, Sabba S. Ştefănescu Institute of Geodynamics, 19–21 Jean Louis Calderon Street, Sector 2, 20032 Bucharest, Romania.

**Abstract:** Extension-related magmatism with arc-like features was active in the South Apuseni Mountains, Romania during the Neogene and Quaternary. The current chronological framework is primarily restricted to K–Ar dates. We present here new laser ablation inductively coupled plasma mass spectrometry U–Pb zircon age data for 20 subvolcanic and volcanic rocks from eight different Cenozoic volcanic–intrusive complexes and from Jurassic and Cretaceous lava flows. Our results support magmatic ages between *c.* 14 and *c.* 7 Ma, with Uroi, an alkaline intrusion, occurring significantly later at *c.* 1.5 Ma. Revising the timeline for the South Apuseni Mountains palaeomagnetic rotations shows that most of the clockwise vertical-axis rotation of these mountains ( $54.4^\circ \pm 10.7^\circ$ ) took place between *c.* 14 and 11 Ma, the age interval when the majority of the magmas were emplaced. Xenocrystic zircon dates show differences in the age populations between individual volcanic–intrusive complexes. A Permo-Triassic population is almost ubiquitous, indicating that basement Permo-Triassic igneous rocks are more widespread than previously thought, or that they were significantly involved in the generation of Neogene magmas. However, other observed age populations, such as Triassic or Paleogene, have no clear correspondence in the known geological record, indicating the presence of a cryptic component interacting with Neogene magmas.

**Supplementary material:** Full analytical details and age calculations for the U–Pb age data collected during this study, rock samples and separated zircon fraction descriptions and the palaeomagnetic and age databases are available at <https://doi.org/10.6084/m9.figshare.c.6951429>

Received 21 April 2023; revised 21 November 2023; accepted 24 November 2023

Extension-related calc-alkaline and alkaline magmatism was active in the Carpathian–Pannonian domain from the Miocene until 30 ka (e.g. Pécskay *et al.* 1995, 2006; Fedele *et al.* 2016; Karátson *et al.* 2016; Molnár *et al.* 2018; Ducea *et al.* 2020) and was generated by the subduction and retreat of a slab, possibly associated with the closure of the Alpine Tethys Ocean (Seghedi and Downes 2011; Ismail-Zadeh *et al.* 2012; Ducea *et al.* 2020). The roll-back process resulted in extensional settings and in the rotation and translation of part of the Dacia crustal block. Centrally located between the Pannonian and Eastern Carpathians domains and at the boundary between the Dacia and Tisza Mega-Units, the South Apuseni Neogene and Quaternary magmatic district represents a key area for understanding the geodynamic evolution of this region.

The emplacement of magmas in the South Apuseni Mountains during the Miocene was promoted by extensional normal faults caused by rotation of the underlying crustal blocks (Pătraşcu *et al.* 1994; Roşu *et al.* 2004a; Seghedi *et al.* 2022). These magmas, ranging from basaltic andesites to dacite in composition, show subduction-related geochemical signatures, with enrichments in large ion lithophile elements and light rare earth elements, troughs at Nb–Ta and Ti, and occasionally high Sr/Y, large ion lithophile

elements and light rare earth elements similar to adakitic rocks (Roşu *et al.* 2001, 2004a; e.g. Harris *et al.* 2013; Seghedi *et al.* 2022). Miocene rocks occur in both volcanic and subvolcanic forms. There are multiple hypotheses about their genesis, ranging from decompression melting of a metasomatized subcontinental lithospheric mantle, melting of eclogitized lower crust and/or uppermost mantle due to interactions with asthenospheric melts, and melting of the retreating slab (Roşu *et al.* 1997, 2001, 2004a; Seghedi *et al.* 2010; Harris *et al.* 2013; Holder 2016; Ducea *et al.* 2020; Seghedi *et al.* 2022).

To date, the duration and age progression of the South Apuseni Neogene and Quaternary magmatism is constrained primarily through K–Ar ages (e.g. Pécskay *et al.* 1995; Roşu *et al.* 1997; Seghedi *et al.* 2022). However, K–Ar dating can yield unreliable dates due to excess <sup>40</sup>Ar caused by the presence of xenocrysts and micro-xenoliths or due to <sup>40</sup>Ar loss caused by post-emplacment hydrothermal activity (Kelley 2002a). Existing zircon U–Pb age values for our study area are mostly limited to intrusions of economic interest (Kouzmanov *et al.* 2005b, 2006; Holder 2016). Zircon U–Pb dating is a key tool in deciphering the emplacement history of magma and the slow diffusion of Pb at magmatic temperatures also makes it

well-suited to record the cryptic crustal components that contribute to melts (e.g. [Cherniak and Watson 2001](#); [Tapster \*et al.\* 2014](#)).

To address the spatiotemporal distribution of the South Apuseni magmatism and its links with crustal rotation, we provide here an updated and revised geochronological framework based on 20 new laser ablation inductively coupled plasma mass spectrometry U–Pb dates and a compilation of 37 published U–Pb and 42 published K–Ar dates. We compare the K–Ar dates with the U–Pb data to assess their utility for geological interpretation. In addition, we present the first analysis of inherited zircon populations in Neogene and Quaternary magmatic rocks to decipher the underlying basement, hidden underneath Jurassic and younger volcanic and sedimentary rocks.

## Regional geology

The Apuseni Mountains are located between two sedimentary basins: the Cenozoic Pannonian Basin to the west and the Late Cretaceous–Cenozoic Transylvanian Basin to the east. The underlying basement is made up of two mega-units, the Tisza and Dacia, and is overlain by the Southern Apuseni ophiolitic unit, which was obducted onto the Dacia Mega-Unit at *c.* 153 Ma ([Gallhofer \*et al.\* 2017](#)) and intruded by Late Cretaceous and Miocene calc-alkaline magmas ([Roşu \*et al.\* 2004a](#); [Seghedi 2004](#); [von Quadt \*et al.\* 2005](#); [Gallhofer \*et al.\* 2015](#); [Vander Auwera \*et al.\* 2016](#); [Seghedi \*et al.\* 2022](#)). The Tisza and Dacia mega-units are made up of nappes that were amalgamated during the Variscan and Alpine orogenies ([Balintoni \*et al.\* 2007, 2010](#); [Reiser \*et al.\* 2017](#)). From the bottom up, these are the Bihor Autochthonous Unit and the Codru nappe system ([Săndulescu 1984](#)), representing the Tisza Mega-Unit, overlain by the Biharia nappe system ([Săndulescu 1984](#)), which is part of the Dacia Mega-Unit ([Fig. 1](#)). These are locally intruded and overlain by Variscan and Permian intrusive and volcanic rocks ([Pană \*et al.\* 2002](#); [Balintoni \*et al.\* 2010](#); [Nicolae \*et al.\* 2014](#); [Szemerédi \*et al.\* 2021](#)).

Overlying the Vidolm nappe are the Transylvanides, a tectonic unit containing fragments of oceanic crust ([Săndulescu 1984](#)) ([Fig. 2](#)) exhibiting subduction-related trace element signatures and ascribed to back-arc and island arc settings ([Bortolotti \*et al.\* 2002](#);

[Nicolae and Saccani 2003](#); [Gallhofer \*et al.\* 2017](#)). These were formed between 159 and 153 Ma and thrust over the Vidolm nappe after 153 Ma ([Gallhofer \*et al.\* 2017](#)), followed by the intrusion of the Late Cretaceous to Early Paleogene ‘banatitic suite’ ([Fig. 2](#)). The latter was related to the closure of the Neotethys Ocean under the Dacia-Tisza Mega-Unit, dated in the Apuseni Mountains by [Gallhofer \*et al.\* \(2015\)](#) to 81 and 75.5 Ma. Fission track data, collected predominantly from the Northern Apuseni Mountains or Late Cretaceous sediment cover, indicate periods of uplift related to the erosional denudation of the domed Bihor nappe system and two previously unknown compressional events during the Early Eocene and Early Oligocene near the Mezeş thrust ([Merten \*et al.\* 2011](#); [Kounov and Schmid 2012](#)). However, the presence of Paleogene alluvial sediments in the South Apuseni Mountains indicates a period of uplift and erosion. ([Roşu \*et al.\* 1997](#)).

## Neogene volcanism

Miocene closure of the Carpathian embayment, generated by the roll-back of an SE–NW-oriented slab, resulted in extensional tectonics ([Burchfiel and Royden 1982](#); [Balla 1987](#); [Maţenco and Radivojević 2012](#)) and the generation of high volumes of calc-alkaline and alkaline magmas in the Pannonian Basin, Eastern Carpathians and South Apuseni Mountains ([Ghiţulescu and Socolescu 1941](#); [Harangi 2001](#); [Roşu \*et al.\* 2004a](#); [Seghedi \*et al.\* 2004, 2022](#); [Harris \*et al.\* 2013](#); [Lukács \*et al.\* 2018](#); [Brek \*et al.\* 2021](#)). According to palaeomagnetic data, this Miocene closure was accompanied by vertical-axis rotation of the Apuseni Mountains ([Pătraşcu \*et al.\* 1994](#); [Roşu \*et al.\* 2004a](#)).

The majority of the magmatic products are andesitic, with minor basaltic andesites, dacites and rhyolites. (e.g. [Roşu \*et al.\* 2004a](#); [Harris \*et al.\* 2013](#)). A detailed description of the analysed samples is reported in Supplementary material, Appendix 1, Section 2. The Neogene magmas exhibit subduction-related signatures, sometimes with an adakitic fingerprint ([Roşu \*et al.\* 2004a](#); [Harris \*et al.\* 2013](#); [Seghedi \*et al.\* 2022](#)), despite being distant from an active subduction zone (the Neogene subduction-associated suites in the Carpathian arc are 200 km east at the present day) and associated with extensional tectonics (e.g.

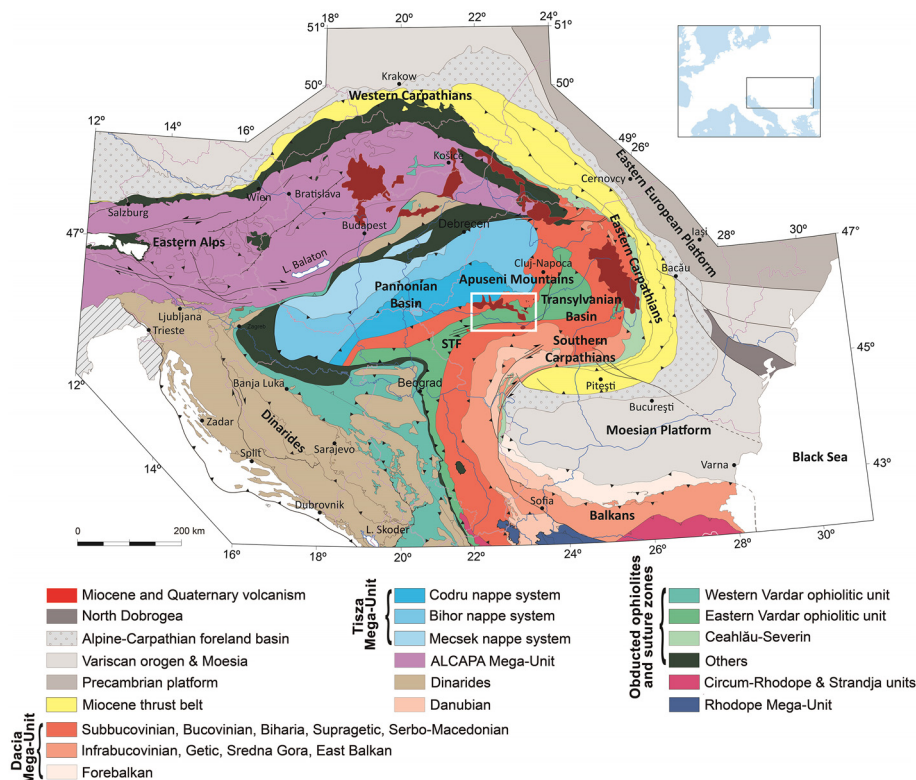


**Fig. 1.** Simplified geotectonic map of the Carpatho-Pannonian region showing the Miocene calc-alkaline magmatism. The white rectangle highlights the study area of the South Apuseni Mountains (see [Fig. 2](#)). STF, South Transylvanian Fault. Source: geotectonic map after [Schmid \*et al.\* \(2008\)](#); calc-alkaline magmatism after [Seghedi \*et al.\* \(2022\)](#).

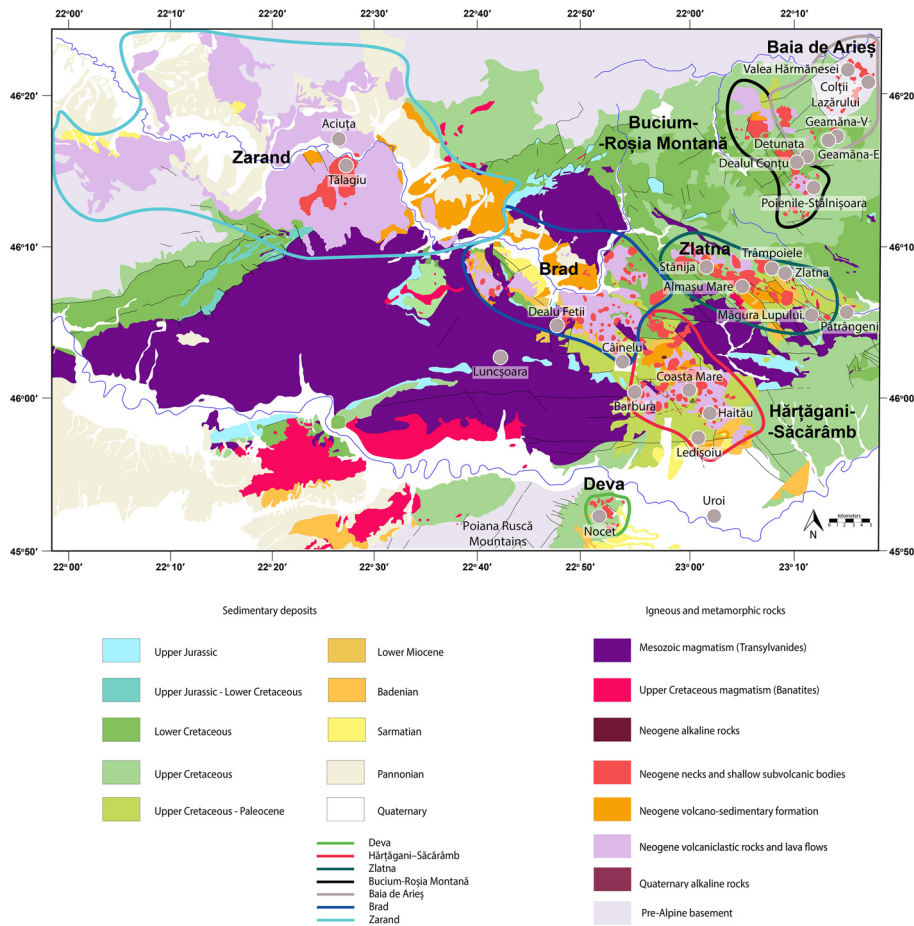


**Fig. 2.** Geological map of the South Apuseni Mountains showing the locations of the collected samples (grey circles). Thick coloured lines represent the volcanic–intrusive complexes as shown in the legend. The Uroi VIC represents only a small intrusive body from where the sample was collected. Source: after Roșu and Nicolae (2001).

Roșu *et al.* 2004a; Harris *et al.* 2013; Seghedi *et al.* 2022). Previous workers have identified a number of different volcanic–intrusive complexes (VICs) – the Baia de Arieș, Bucium–Roșia Montană, Zlatna, Brad, Zarand, Hărtăgani–Săcărâmb, Deva and Uroi VICs (Fig. 2; Roșu *et al.* 2004b) – and this nomenclature is also used here.

Based on existing K–Ar and U–Pb radio-isotopic dating, magmatism is considered to have been active between 14.8 and 7.4 Ma (Roșu *et al.* 1997, 2004a, b; Kouzmanov *et al.* 2005a, b; Holder 2016; Seghedi *et al.* 2022). The earliest magmatic products can be found in the Bucium–Roșia Montană VIC and magmatic activity slowly migrated westwards and southwards with time. After 10.5 Ma, the volcanic activity around Baia de Arieș produced magmas with distinct geochemical features, such as higher large ion lithophile element contents and more mantle-like Sr and Nd isotopic signatures (Roșu *et al.* 2004a, b; Harris *et al.* 2013; Seghedi *et al.* 2022), until 7.4 Ma, when Miocene activity ceased (Roșu *et al.* 2004a). The last magmatic manifestation recorded in the South Apuseni Mountains is the small alkaline intrusion from Uroi, previously dated at 1.6 Ma by the K–Ar method (Pécskay *et al.* 1995).

Current hypotheses regarding the source of the South Apuseni Neogene and Quaternary magmas include a subcontinental lithospheric mantle metasomatized during previous subduction events (Roșu *et al.* 2004a; Harris *et al.* 2013), lower crust/uppermost mantle mixed with various mantle melts (Seghedi *et al.* 2022) or the retreating slab (Ducea *et al.* 2020).

### Sample selection and analytical techniques

Fresh to minimally altered rock samples were collected from Neogene VICs and two Jurassic and two Cretaceous rhyolitic lava flows. The sample locations are detailed in Table 1 and Figure 2.

Heavy mineral separates were obtained at the Geochronology and Tracers Facility, British Geological Survey (Keyworth, UK). At

least 3 kg of rock sample were crushed using a jaw-crusher and ground using a disc mill. Samples were then sieved and the heavy minerals were separated using a Rogers table, a Franz electromagnetic separator and diiodomethane heavy liquid. The zircon fraction was hand-picked under a binocular microscope and mounted in an epoxy mount, which was then polished with 0.25 μm diamond paste. Back-scattered electron and cathodoluminescence imaging of the separated zircon crystals was undertaken at the University of Leicester (Leicester, UK) using a Deben Centaurus cathodoluminescence detector mounted on a Zeiss Sigma 300 analytical scanning electron microscope. The operating conditions for the scanning electron microscope were 15 kV, 50 μA and an 11–13 mm working distance. The samples were repolished and cleaned after imaging.

U–Pb data were obtained at the British Geological Survey Geochronology and Tracers Facility using a Nu Instruments Nu Plasma HR multi-collector inductively coupled plasma mass spectrometer equipped with a New Wave Research 193ss laser ablation system. Ablation spots (*c.* 15 μm depth with diameters of 35 and 25 μm for the crystal rims and cores, respectively) were chosen based on the cathodoluminescence and back-scattered electron images and optical microscopy. A fluence between 1.5 and 2.5 J cm<sup>-2</sup> and an ablation frequency of 5 Hz were used. Corrections for initial <sup>230</sup>Th disequilibrium were applied following the method detailed in Tapster *et al.* (2016), resulting in an additional *c.* 90 kyr on each age interpretation. More details regarding the methodology can be found in Supplementary material, Appendix 1, Section 1.

### Characterizing zircon populations and interpreting age data

Various types of zircon crystals have been recognized in the investigated rock samples, for which we adopted the terminology of Miller *et al.* (2007). Antecrysts are defined as zircons that

**Table 1.** Calculated (including initial  $^{230}\text{Th}$  disequilibrium corrections) emplacement ages for the investigated rocks from the South Apuseni Mountains, including sample locations and geographical coordinates

Volcanic–intrusive complex	Rock sample	Location	°E	°N	Age (Ma)	Error ( $\pm$ Ma)
Bucium–Roşia Montană	CON-01	Dealul Conţu	23.18261	46.26082	13.39	0.19
	POI-01	Poienile - Stâlnişoara	23.21009	46.23131	13.33	0.25
Baia de Arieş	BR-01	Valea Hărmănesei	23.27277	46.35965	9.26	0.16
	SIM-02	Colţii Lazărului	23.30987	46.35111	8.77	0.06
	DET*	Detunata	23.20333	46.26611	8.57	0.52
	GEA-E	Geamăna-Est	23.24677	46.28546	8.35	0.06
	GEA-V	Geamăna-Vest	23.23617	46.28138	7.33	0.06
Zarand	ACI*	Aciuţa quarry	22.4507	46.2942	12.69	0.23
					12.07	0.22
Zlatna	TLG	Tălagiu quarry	22.46305	46.27059	12.2	0.15
	STN-09g	Corbu stream, Stăniţa	23.04415	46.14413	12.61	0.08
	MLP-01	Măgura Lupului quarry	23.17616	46.09209	12.05	0.12
	TRP-03	Trâmpoiele	23.13915	46.14376	12.43	0.1
	AM-04g	Neagra quarry, Almaşu Mare	23.09023	46.1243	12.79	0.06
Brad	DFT-02g	Dealul Fetii	22.79565	46.08466	11.71	0.06
	CIN	Câinelu de Sus	22.890145	46.053465	12.94	0.08
Hărtăgani–Săcărâmb	HAI-01	Haitău	23.03055	45.97829	10.41	0.1
	PT-01	Coasta Mare	23.01252	46.00174	10.86	0.07
	LED	Ledişoii	23.01383	45.95325	10.4	0.08
Deva	NUC-02	Nocet hill	22.85296	45.86763	11.53	0.09
Uroi	UR-01	Uroi Hill	23.04499	45.85616	1.54	0.05
Cretaceous	PAT	Pătrângenii rhyolite	23.258	46.09203	82.12	0.5
	ZLT	Zlatna	23.20183	46.11808	81.78	0.64
Jurassic	LUN	Luncşoara	22.70238	46.04466	161.24	0.8
	BAR	Barbura	22.90932	46.00722	163.06	0.9

Errors are  $2\sigma$ . Emplacement ages for samples marked with an asterisk represent lower intercept TW Concordia ages. The Zarand sample from the Aciuţa quarry displays two clearly distinct populations.

crystallized from an earlier pulse of magma and were incorporated in a later pulse, whereas crystals whose relation with the final magma fraction and emplacement is certain are named autocrysts. Xenocrysts are crystals sourced from a host rock that is distinctly older than the magmatic system. They can be found either as inherited cores or individual crystals and can be easily distinguished due to their different cathodoluminescence response, rounded edges and resorption features. A crystal may therefore have multiple xenocrystic cores, antecrystic growth zones and autocrystic rims.

We analysed zircon crystals from 24 rock samples, 20 belonging to the Neogene and Quaternary magmatism and four from the Cretaceous and Jurassic basement. Weighted mean ages of  $^{206}\text{Pb}/^{238}\text{U}$  were calculated from analyses that showed  $>95\%$  concordance between  $^{206}\text{Pb}/^{238}\text{U}$  and  $^{207}\text{Pb}/^{235}\text{U}$  and were considered relevant if their  $2\sigma$  mean square weighted deviation was  $\leq 1 + 2(2/f)^2$  (Wendt and Carl 1991), where  $f$  represents degrees of freedom (number of analyses  $- 2$ ). Where the weighted mean ages could not be calculated (e.g. due to high common Pb), lower intercept ages from Tera Wasserburg projections were considered. Full results are presented in Table S1. Individual U–Pb crystallization ages with their corresponding cathodoluminescence images are discussed for each rock sample in Supplementary material, Appendix 1, Section 2.

Probability density plots were constructed using DensityPlotter (Vermeesch 2012). For crystals displaying ages younger than 1200 Ma, the probability density plots were constructed using  $^{206}\text{Pb}/^{238}\text{U}$  ages for analyses showing a  $>90\%$  concordance between  $^{206}\text{Pb}/^{238}\text{U}$  and  $^{207}\text{Pb}/^{235}\text{U}$ . For samples with ages older than 1200 Ma,  $^{207}\text{Pb}/^{206}\text{Pb}$  ages were preferred.

## Results

### Zircon characterization

The zircon crystals in the analysed samples show diverse morphologies, ranging from euhedral to subhedral with a minor

population of anhedral crystals (Fig. 3). The majority are prismatic, but more elongated or rounded zircons are also common, such as crystals 1 and 4 (Fig. 3a). Broken fragments are found in almost all samples. Crystals range in size from  $<20$  to  $400\ \mu\text{m}$ . The majority of crystals show fine oscillatory zoning, commonly overprinted by sector zoning; patchy or banded zoning has also been observed (Fig. 3). Inherited cores are common and can easily be discerned due to their different cathodoluminescence response relative to the rims. They are usually rounded, exhibiting resorption features at the core–rim interface and faint sector or oscillatory zoning (Fig. 3b). They vary between 10 and  $>100\ \mu\text{m}$  in diameter. Zircon crystals with multiple cores or xenocrystic crystals with older cores (crystal 1, Fig. 3b) were also observed.

### U–Pb dates and age interpretations of Neogene and Quaternary zircon populations

The Neogene and Quaternary zircon populations exhibit dates ranging from 18.15 to 1.54 Ma. The interpreted Neogene crystallization ages range mainly from  $13.4 \pm 0.2$  to  $7.3 \pm 0.1$  Ma. A significantly younger age was obtained for a rock sample from the Uroi complex of  $1.5 \pm 0.1$  Ma. Age interpretations are summarized in Table 1 and Fig. S1 and a more detailed description of the workflow for each rock sample can be found in Supplementary material, Appendix 1, Section 2.

Eight samples yielded dates that were significantly older than their interpreted emplacement ages, but belonged to the same time interval and magmatic activity. These can be interpreted as due to the presence of antecrystic or xenocrystic zircon crystals, the latter related to shallow crustal contamination from eroded or currently undated intrusions or volcanic rocks in their vicinity. For example, in the Baia de Arieş VIC, the Geamăna-E intrusion ( $8.4 \pm 0.1$  Ma) contains zircon crystals with dates ranging back to 14.6 Ma and the nearby Geamăna-V body ( $7.3 \pm 0.1$  Ma) shows an almost continuous distribution of dates from 8.9 to 7.1 Ma (Fig. 4). A presentation of

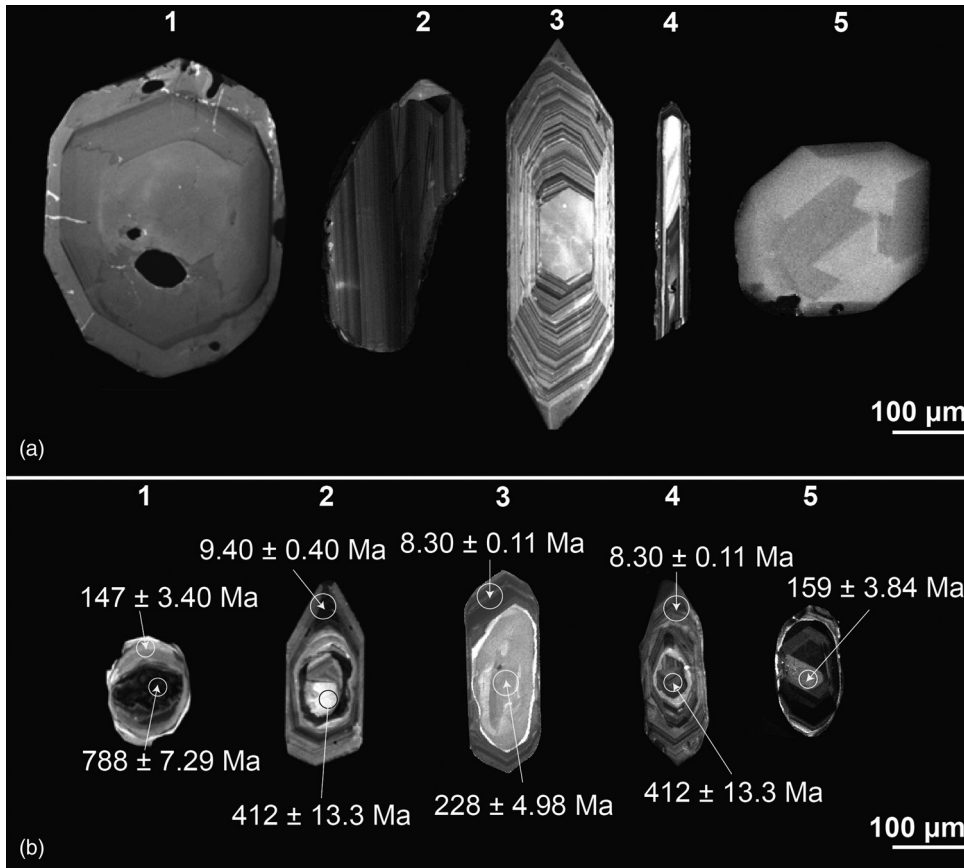


**Fig. 3.** Cathodoluminescence images showing the diverse morphologies of the zircon crystals found in the investigated Neogene and Quaternary rocks from the South Apuseni Mountains. (a) Crystals segregated from the host magma: 1, rounded subhedral zircon crystal with faint oscillatory zoning; 2, anhedral, possibly resorbed crystal; 3, euhedral prismatic crystal with strong oscillatory zoning; 4, elongated crystal with oscillatory and sector zoning; 5, anhedral crystal exhibiting sector zoning. (b) Various inherited crystals and cores, including the analysed dates: 1, resorbed xenocrystic crystal with older xenocrystic core; 2, 3, 4, xenocrystic cores exhibiting resorption features with Neogene magmatic overgrowths; 5, xenocrystic core with thin magmatic overgrowth. Crystals a1 and b5 are from a rock sample in the Zarand volcanic–intrusive complex (VIC); crystals a2, b3, a4, b4 and b2 were extracted from rock samples from the Baia de Arieş VIC. Crystal a5 was obtained from a rock sample from the Uroi VIC and crystal a3 from a rock sample collected from the Hărţăgani–Săcărâmb VIC.

antecrystic zircon data is given alongside the age interpretations in Supplementary material, Appendix 1, Section 2.

**Comparison between our U–Pb data and previously published K–Ar age data**

Ideally, K–Ar dates should document indistinguishable or slightly younger dates, as a result of the lower closure temperature, than the youngest zircon U–Pb dates from the same sample. However, K–Ar ages can be affected by Ar loss, Ar gain, inherited Ar from crustal assimilation or xenoliths (Kelley 2002a, b; Hora et al. 2010). Unlike zircon, the minerals or rocks used for K–Ar dating are particularly susceptible to disturbance from hydrothermal alteration and weathering, thus posing significant questions about their significance (Kelley 2002b). To assess the reliability of the existing K–Ar data for the South Apuseni igneous rocks, we determined zircon U–Pb ages for seven samples previously dated using the K–Ar method (Fig. 5).

One of the oldest samples in the Bucium–Roşia Montană VIC provides a U–Pb age of  $13.3 \pm 0.3$  Ma compared with  $14.6 \pm 1.6$  Ma by the K–Ar method (Roşu et al. 1997). New U–Pb ages for rock samples in the Zlatna ( $12.4 \pm 0.1$  Ma), Hărţăgani–Săcărâmb ( $10.9$

$\pm 0.1$  Ma) and Uroi ( $1.5 \pm 0.1$  Ma) VICs are also within the uncertainty of previous K–Ar ages ( $12.6 \pm 0.5$ ,  $10.4 \pm 0.4$  and  $1.6 \pm 0.1$  Ma, respectively). However, it is evident that the U–Pb method provides relatively higher precision. Significant differences, larger than the  $2\sigma$  reported uncertainties, have also been observed, especially in samples from the Zlatna ( $12.79 \pm 0.06$  v.  $11.07 \pm 0.63$  Ma), Baia de Arieş ( $7.3 \pm 0.1$  v.  $7.8 \pm 0.3$  Ma) and Deva ( $11.5 \pm 0.1$  v.  $12.6 \pm 0.5$  Ma) VICs. No consistent or systematic difference is observed, suggesting that multiple causes were responsible for the observed age differences obtained using the two methods.

Despite the significant differences in dates, the relative sequencing of events is unchanged from the K–Ar to U–Pb ages, suggesting that the K–Ar ages can be meaningfully interpreted and can still provide chronological insights within the *c.* 7 Myr evolution of the Neogene magmatism, albeit with caveats on their stated uncertainties.

**Jurassic and Cretaceous samples**

The analysed Jurassic and Cretaceous rock samples were dated to  $161.2 \pm 0.8$  and  $163.1 \pm 0.9$  Ma and to  $82.1 \pm 0.5$  and  $81.8 \pm 0.6$  Ma, respectively (Table 1, Fig. S1).

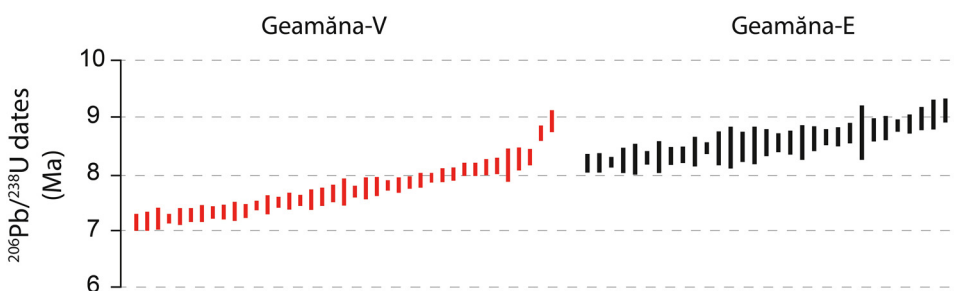


**Fig. 4.** Distribution of geochronology dates for individual zircon crystals in the Geamăna-V and Geamăna-E andesites, part of the Baia de Arieş volcanic–intrusive complex. Solid bars represent the  $2\sigma$  uncertainties of the analyses. The 14 Ma dates for the Geamăna-E sample are not shown.

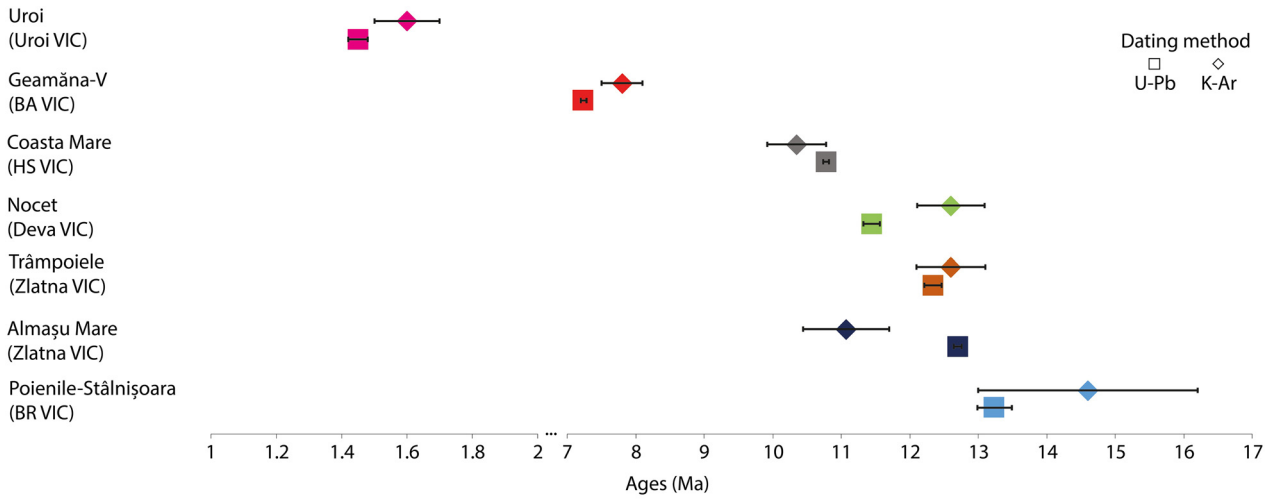


**Fig. 5.** Comparison between literature K–Ar data (Pécskay *et al.* 1995; Roșu *et al.* 1997) and the zircon U–Pb age data from this study collected from the same localities/intrusions. Horizontal lines represent error bars. Ages in Ma are shown on the x-axis, whereas the y-axis displays the locality/intrusion name and the volcanic–intrusive complex. BA, Baia de Arieș; HS, Hărtăgani–Săcărâmb; BR, Bucium–Roșia Montană.

### Xenocrystic zircon populations

The studied Neogene samples contain numerous pre-Neogene zircon crystals, either as xenocrysts or cores surrounded by younger rims (Fig. 3b). The number of inherited zircon crystals varies significantly between individual samples, ranging from 91 to only two crystals. Samples from the Baia de Arieș VIC contain, on average, more

xenocrystic crystals and cores. The distribution of xenocrystic age data for all the investigated VICs is shown in Figure 6. The sample from Uroi exhibits populations from the Late Eocene, Early Paleocene, Late Cretaceous, and Early and Late Permian. Zircon crystals from the nearby Deva VIC fall within the Late Cretaceous and Neoproterozoic. Xenocrysts from Zarand exhibit ages belonging to the Archean, Proterozoic, Devonian–Carboniferous (the largest

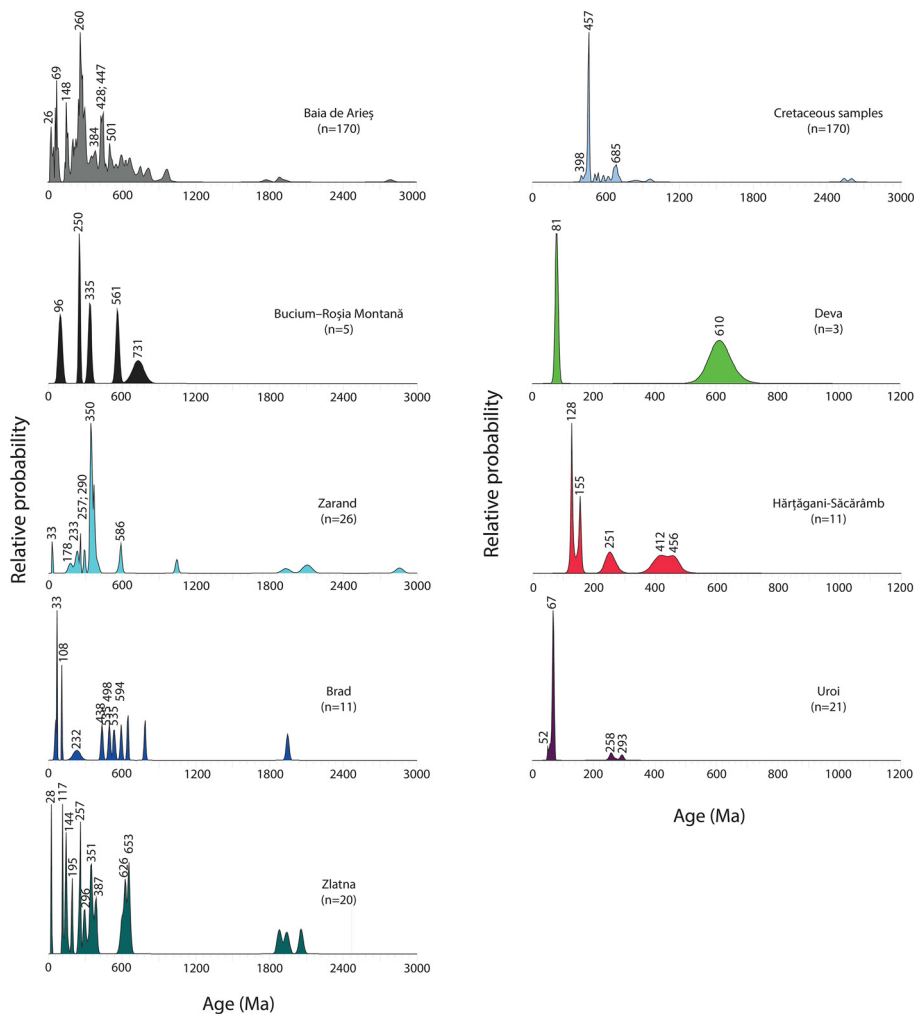


**Fig. 6.** Probability density plots of U–Pb age data obtained for xenocrystic zircon crystals and cores from the investigated South Apuseni Mountains volcanic–intrusive complexes; *n* refers to the number of analysed crystals. Colours for the various volcanic–intrusive complexes as in Figure 2.

population), Permo-Triassic, Early Jurassic and Oligocene, whereas additional populations of (mostly) Neoproterozoic and (subordinate) Early Cretaceous ages have been observed in the Zlatna VIC. Samples from Brad are similar, exhibiting, in addition, Late Cretaceous and Paleocene populations. In the Hărăgani–Săcărâmb VIC, the analysed xenocrysts, albeit scarce, span a wide range from the Ordovician to the Early Devonian, Triassic, Early Jurassic and Early Cretaceous. Rock samples from the Bucium–Roșia Montană VIC display a population of Neoproterozoic, Devonian–Carboniferous, Permo-Triassic and Late Cretaceous xenocrystic crystals. Samples belonging to the Baia de Arieș VIC exhibit the largest population of xenocrystic zircon crystals, with significant age groups belonging to the Permo-Triassic, Ordovician–Silurian, Cretaceous and Late Jurassic (Fig. 6). Cretaceous samples exhibit an important Late Ordovician population and minor Cambrian, Neoproterozoic and Archean populations. No inherited zircon crystal was found in the analysed Jurassic samples.

## Discussion

### Updated timeline for vertical axis rotations in the South Apuseni Mountains

Evidence for vertical axis rotations based on palaeomagnetic data from Tertiary magmatic rocks from the South Apuseni Mountains (Pătrașcu *et al.* 1994; Roșu *et al.* 2004a) has been used in several tectonic models of the Carpathians (e.g. van Hinsbergen *et al.* 2020 and references cited therein). However, the limitations of the existing K–Ar dates in terms of precision and accuracy generate uncertainty within these prior interpretations. Based on the numerous recent U–Pb ages (Kouzmanov *et al.* 2005a, b; Gallhofer *et al.* 2015; Holder 2016; this study), we refine the timeline for the vertical axis rotations in the South Apuseni Mountains, as inferred by palaeomagnetic data. The sites where palaeomagnetic data were obtained (Pătrașcu *et al.* 1994; Roșu *et al.* 2004a) have been divided into four groups based on the available ages (Table S3; Fig. S2). For each group, we calculated the mean age based on the U–Pb ages and, in their absence, on the available K–Ar ages. We calculated the mean palaeomagnetic direction based on Fisher (1953) statistics. To ensure that the mean palaeomagnetic directions can be used for tectonic interpretation, we followed the criteria of van Hinsbergen *et al.* (2020): (1)  $k$  values (Fisher 1953)  $\geq 50$ ; (2) a fixed  $45^\circ$  cut-off angle from the mean palaeomagnetic pole; and (3) at least four sites can be averaged from an area.

The first group includes five sites sampled from the magmatic rocks of the Late Cretaceous (banatitic suite) related to the closure of the Neotethys Ocean under the Dacia-Tisza Mega-Unit, which were considered to be of Eocene–Oligocene age by Pătrașcu *et al.* (1994). The available U–Pb ages from the South Apuseni Mountains (Gallhofer *et al.* 2015; this study) and the K–Ar age from Downes *et al.* (1995) indicate that the age of these magmatic rocks is Late Cretaceous. If we take these U–Pb ages into account, then the mean age of the rock samples from this group is  $79.8 \pm 1.6$  Ma (seven ages between 82.0 and 77.8 Ma). The second group includes 15 sites where Miocene magmatic rocks crop out with a mean age of  $13.3 \pm 0.6$  Ma (eight ages between 14.8 and 12.8 Ma). The third group comprises 37 sites characterized by igneous rocks with a mean age of  $11.6 \pm 0.8$  Ma (19 ages between 12.8 and 10.3 Ma). The fourth group contains six sites where igneous rocks yielded a mean age of  $8.5 \pm 0.9$  Ma (six ages between 9.4 and 7.3 Ma).

The presence of antipodal normal and reversed directions in the Miocene groups indicates that the sampling covers enough time to average the secular variation to yield a mean direction that can be used for tectonic interpretation. The second and the third groups also have a positive reversal test (McFadden and McElhinny 1990)

classification C (observed angle  $10.0^\circ$  less than the critical angle  $13.2^\circ$ ) and classification B (observed angle  $1.1^\circ$  less than the critical angle  $8.8^\circ$ ), respectively.

We used the method of Debiche and Watson (1995) to compute the amplitude of vertical axis rotations. The mean palaeomagnetic directions for the third and fourth groups are close to that of a geocentric axial dipole at the sampling area (Fig. 7). We interpret these results as indicating the absence of vertical axis rotations after 11.6 Ma, so we took the mean palaeomagnetic direction for 11.6 Ma as a reference for the amplitude of vertical axis rotations. The amplitude of rotation between 79.8 and 11.6 Ma is  $64.8 \pm 11.6^\circ$ . This value is comparable with those obtained for Late Cretaceous rocks from the Apuseni Mountains ( $83.3 \pm 6.5^\circ$ ) and the South Carpathians ( $70.1 \pm 10.4^\circ$  and  $85.2 \pm 11.4^\circ$ ; Panaiotu and Panaiotu 2010). The amplitude of vertical-axis rotation between 13.3 and 11.6 Ma is  $54.4 \pm 10.7^\circ$ . These results confirm that most of the clockwise rotation of the Tisza-Dacia Block was rapid, taking about 2–3 Myr (e.g. Roșu *et al.* 2004a). The estimated amplitude of the vertical-axis rotation agrees with the reconstruction of the Miocene kinematic evolution of the Carpathian area provided by van Hinsbergen *et al.* (2020).

### Revised chronological framework for Neogene and Quaternary magmatism in the South Apuseni Mountains

Based on the 57 available U–Pb ages (Table S2), Neogene magmatism in the South Apuseni Mountains was active between at least  $13.7 \pm 0.6$  Ma (Bucium–Roșia Montană VIC) and  $7.3 \pm 0.1$  Ma (Baia de Arieș VIC, Fig. 8). Magmatic activity prior to the dated samples is also recorded in the antecrystic population exhibiting ages up to 14.5 Ma in the Baia de Arieș, Bucium–Roșia Montană and Zlatna VICs and in some of the K–Ar ages (Fig. 8, Table S2). There does not seem to be any preferential east–west migration of magmatic activity with time, with centres in the far west (Zarand) being relatively coeval with those in the east

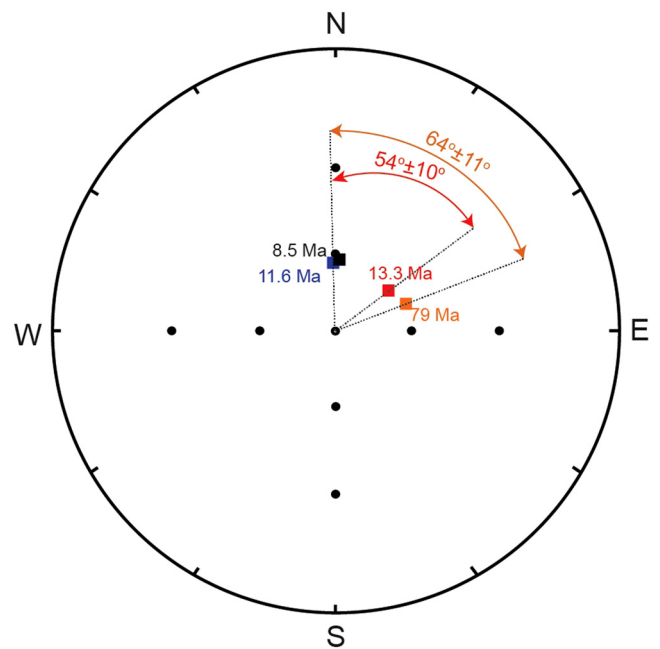


**Fig. 7.** Mean palaeomagnetic directions for the Late Cretaceous (orange line and corresponding value) and Miocene group 1 (red line and corresponding value) magmatic rocks from the South Apuseni Mountains. The amplitudes of the vertical axis rotations are computed with respect to the 11.6 Ma mean palaeomagnetic directions. The coloured squares and associated ages represent the mean ages of the groups as defined in the text: orange, group 1; red, group 2; blue, group 3; black, group 4.

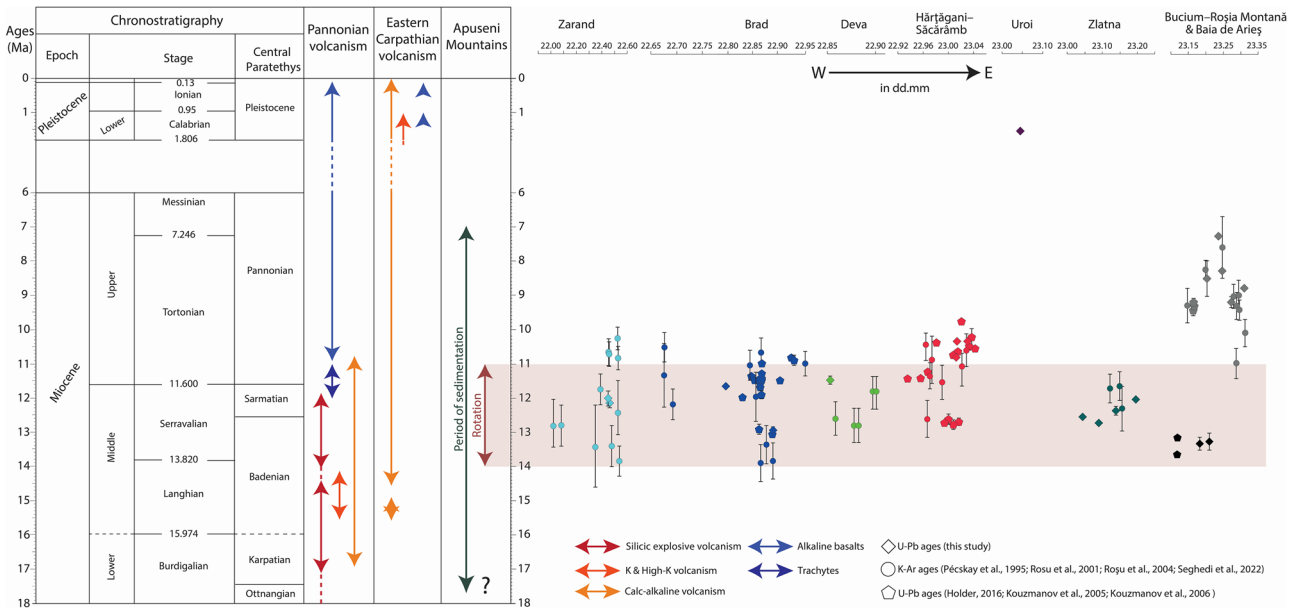


**Fig. 8.** Spatial and temporal evolution of Neogene magmatism in the Apuseni Mountains. U–Pb ages from this study, Holder (2016), Kouzmanov *et al.* (2005b) and Kouzmanov *et al.* (2006). K–Ar ages from Pécskay *et al.* (1995), Roşu *et al.* (2001), Roşu *et al.* (2004a, b) and Seghedi *et al.* (2022). Temporal scale and Pannonian magmatism after Balázs *et al.* (2016) and Harangi (2001). More details regarding Pannonian magmatism and its geochemical characteristics can be found in Harangi (2001). Eastern Carpathian magmatism after the compilation by Vlasceanu *et al.* (2021). Colours for the various volcanic–intrusive complexes as in Figure 2. The black vertical lines are error bars. Dd.mm indicates that the values are in degrees and minutes. The database for the figure can be found in Table S2.

(Zlatna) or in the centre (Brad, Fig. 8). The most prolific time for magma generation was during crustal rotation (Fig. 8).

The geochronological data for individual VICs in the South Apuseni Mountains show evidence for episodic magmatic activity (Fig. 8). For example, the Hărtăgani–Săcărâmb VIC displays three main periods of flare-ups lasting between c. 150 and 600 kyr and lulls from c. 1 Myr to c. 300 kyr. In the northernmost South Apuseni Mountains, the oldest Bucium–Roşia Montană VIC was active for c. 500 kyr, followed by small, sporadic and localized intrusions after a pause of >2 Myr in the Baia de Arieş VIC. Based on the distribution of existing geochronological data and the spatial distribution of known Neogene and Quaternary bodies, we can exclude any sampling bias and conclude that the observed intermittent activity is probably linked to the incremental opening of extensional basins, crustal rotation, and compression and extension in the Eastern Carpathians and Pannonian Basin (Seghedi *et al.* 2022).

The youngest intrusion is the small alkaline potassic body cropping out in the Uroi VIC, which was dated in this study at  $1.5 \pm 0.1$  Ma (Fig. 8). Roughly coeval alkaline magmatism was active at the Perşani Volcanic Field (Eastern Carpathians) between 1.2 and 0.68 Ma (Panaiotu *et al.* 2013) and at the eastern extremity of the Pannonian Basin at c. 2.5 Ma (Lucareţ), c. 2 Ma (Bar) and c. 1 Ma (Gătaia; Harangi *et al.* 1995; Pécskay *et al.* 1995; Seghedi *et al.* 2008). Nevertheless, there is no clear link between these events.

### Crustal components in the South Apuseni Mountains

Two major tectonic units underlie the South Apuseni Mountains: the Dacia and Tisza mega-units (Fig. 1). These are part of the Inner Carpathian Units (Ducea *et al.* 2018) and were formed as island arcs in a peri-Gondwanan setting from the Late Neoproterozoic to the Ordovician–Silurian (Balintoni *et al.* 2010, 2014; Balintoni and Balica 2013), with an flare-up in magmatic activity at c. 460 Ma (Stoica *et al.* 2016). Zircon populations from these units exhibit major peaks in the Cambrian and Ordovician, with minor inheritance of Neoproterozoic and older zircon populations (Balintoni *et al.* 2010; Ducea *et al.* 2018). The boundaries of the Dacia and Tisza mega-units are obscured by overlying Jurassic back-arc and island

arc products obducted on top of the Dacia and Tisza mega-units during the Late Kimmeridgian (Gallhofer *et al.* 2017).

Other notable features observed in the local geology are Variscan granitoids and metamorphic rocks, including mica schists, ortho- and paragneisses and metabasites (Pană *et al.* 2002; Balintoni *et al.* 2007, 2009), the products of a Permian bimodal magmatic event generated due to the Variscan orogenic collapse and the initiation of Permo-Jurassic extension (Seghedi 2011; Nicolae *et al.* 2014; Szemerédi *et al.* 2020, 2021), and a number of Late Cretaceous intrusions and volcanics (Gallhofer *et al.* 2015; Vander Auwera *et al.* 2016).

Here, we examine the use of inherited zircon crystals within magmatic rocks to better constrain the nature of the crust beneath magmatic centres. Of all the analysed rocks, the xenocrystic populations from the Cretaceous rocks are consistent with those reported in previous studies of the underlying basement (Balintoni *et al.* 2010) and of detrital zircons from rivers flowing through the Dacia terranes (Ducea *et al.* 2018), showing a significant peak at c. 457 Ma and minor inheritance from Neoproterozoic and older zircon crystals. Even though similar populations are observed in samples from other VICs (e.g. Ordovician populations have also been found in samples from the Baia de Arieş and Hărtăgani–Săcărâmb VICs), the main peaks are different, with clear regional differences in xenocrystic populations between VICs.

These differences will be addressed more in detail in the following sections, with the aim of proposing some correlations between the rock units making up the underlying basement.

### Permo-Triassic

One of the most frequently observed xenocrystic zircon populations in the analysed rock samples from the South Apuseni Mountains dates back to c. 260 Ma and is particularly present in the rock samples from the Baia de Arieş VIC (Fig. 6). Locally, early (c. 290 Ma, Balintoni *et al.* 2009) and Mid-Permian (c. 280–260 Ma, Pană *et al.* 2002; Szemerédi *et al.* 2020; Szemerédi *et al.* 2021) intrusions and volcanic rocks crop out in the western Apuseni Mountains and the Pannonian Basin, representing the last stages of



the Variscan collision and the ensuing orogenic collapse. Similarly, late Permian ages have been observed in the Danubian domain (Balintoni and Balica 2012).

No Triassic rock has been described in the investigated area, but a Mid-Triassic zircon population (>237 Ma) has been described in Upper Cretaceous sedimentary rocks from the western Apuseni Mountains (Zaharia *et al.* 2018). However, the Lower Cretaceous Bozeş sedimentary formation (eastern South Apuseni Mountains) exhibits no Permo-Triassic population (Bălc and Zaharia 2013). Few Triassic dates are reported for the Vința granite in the Baia de Arieş VIC (Pană *et al.* 2002), albeit as a highly discordant fraction due to Pb loss, and within the Early Permian Muntele Mare granite, a few kilometres north from the Baia de Arieş VIC in the North Apuseni Mountains (Balintoni *et al.* 2009). Triassic magmatic rocks are found in North Dobrogea (Saccani *et al.* 2004) and at Ditrău (Pál-Molnár *et al.* 2021), >150 km to the east, and Permian and Triassic magmatic rocks have been reported in drill cores from the Moesian Platform (Paraschiv 1978; Paraschiv *et al.* 1983). Hoeck *et al.* (2009) describe a suite of ultramafic to intermediate rocks found as blocks in the Late Barremian–Early Aptian Wildflysch sediments of the Eastern Carpathians, which they interpret as an eroded ophiolitic sequence formed during the Mid- to Late Triassic in an ocean setting bordering the North Apuseni crustal blocks.

#### Devonian–Carboniferous

The Variscan Orogeny is marked by granite and migmatite formation and high-grade metamorphism in the Carpathians, including the Apuseni Mountains (Drăgușanu and Tanaka 1999; Pană *et al.* 2002; Medaris *et al.* 2003; Balica *et al.* 2008). In the investigated samples, Variscan zircons (Fig. 6) represent the main peak in Zarand (*c.* 350 Ma) and minor peaks in Baia de Arieş (*c.* 355 Ma), Zlatna (*c.* 348 Ma) and Bucium–Roșia Montană (*c.* before 339 Ma).

#### Jurassic and Cretaceous

Jurassic back-arc and island arc magmatism was active between 163 and 153 Ma (Gallhofer *et al.* 2017; this study). However, most of the Jurassic dates obtained from the analysed xenocrystic zircon crystals show younger ages (*c.* 150 Ma). A similar trend can be seen for the Cretaceous inherited populations, which show younger (73 Ma in the northern VICs and 67 Ma at Uroi) or older (136 and 112 Ma in the northern VICs and 124 Ma in the southern VICs) dates than the local Cretaceous magmatism, dated to between 82 and 75.5 Ma (Gallhofer *et al.* 2015). A basaltic andesite intrusion near Deva was dated by Downes *et al.* (1995) to 66 Ma, but seems improbable as a possible source.

#### Paleogene

Xenocrystic zircon populations with ages between 66 and 20 Ma have been observed, mainly in samples from the Baia de Arieş, Uroi and Zarand VICs (Fig. 6). No coeval magmatism is known in the South Apuseni Mountains.

#### Provenance of xenocrystic zircon populations

The crustal blocks into which the Neogene and Quaternary magmas of the South Apuseni Mountains intruded exhibit complex geological histories, spanning the Late Cambrian–Miocene time interval (Balintoni *et al.* 2010). However, pre-Jurassic lithologies are covered by Jurassic back-arc and island arc suites and various Cretaceous to Quaternary sediments (Ianovici *et al.* 1976; Seghedi 2004).

The porphyritic nature and intermediate to evolved composition of the investigated South Apuseni Mountains rock samples suggests

ponding in crustal reservoirs, making crustal contamination likely. However, existing Sr–Nd isotope data (Roșu *et al.* 2004a; Seghedi *et al.* 2007, 2022; Harris *et al.* 2013) indicate low degrees of crustal contamination, especially for samples rich in inherited zircon crystals from Baia de Arieş and Zarand, indicating a juvenile source (Roșu *et al.* 2004a, b; Seghedi *et al.* 2007, 2022; Harris *et al.* 2013). A subset of xenocrystic zircon crystals was found rimmed by >35 μm thick Neogene–Quaternary overgrowths, evidence of a long residence time in a Zr-saturated melt. The second subset, showing thin or barely observable rims, indicates late-stage upper crustal contamination or shielding inside xenoliths or xenocrysts.

Although part of the inheritance can be explained through interaction with the crust, not all of the observed xenocrystic zircon populations have any correspondence with the rock units comprising the crustal blocks, requiring input from other sources. The paucity of evidence for occurrence of Triassic, Late Jurassic–Early Cretaceous or Paleogene geological units in the South Apuseni Mountains presents an issue for the argument that zircon inheritance reflects relatively straightforward crustal contamination from the local basement (Fig. 9). This is discussed in the following sections by presenting three possible scenarios.

#### Upper crustal contamination with sedimentary rocks

As shown in Figure 2, some of the analysed samples belong to bodies intruding into sedimentary rocks, especially in the Baia de Arieş. Existing datasets of detrital zircon in Cretaceous sedimentary rocks exhibit important populations of Late Cretaceous (*c.* 82 Ma), Permian (significant populations between 255 and 269 Ma and at 280 Ma), Devonian (380 Ma) and Ordovician (at *c.* 452, 470 and 480 Ma; Zaharia *et al.* 2018) ages, which do not explain the xenocrystic complexity. In addition, the observed Paleogene zircon population in samples from the Baia de Arieş VIC are younger than the surrounding basement units.

#### Presence of cryptic intrusions at depth

Permian intrusions and volcanics crop out, in order of abundance, in the Codru and Biharia nappe systems and in the Bihor Autochthonous Unit (Szemerédi *et al.* 2021), which lie underneath the Baia de Arieş and Vidolm nappes into which the Baia de Arieş magmas intruded. It therefore seems reasonable that Neogene magmas might have interacted with Permian lithologies at depth. However, in the Uroi VIC and in the southern part of the Hărtăgani–Săcărâmb VIC, magmas intrude into the Padeș metamorphic series, part of the South Carpathian/Getic domain (Balintoni *et al.* 2014), where Permian rocks are scarce (Ducea *et al.* 2018).

#### Derivation of xenocrystic zircon populations from the retreating slab

A third possibility is the derivation of the observed xenocrystic zircon populations from the retreating slab. The nature and age of the slab is debated, but Ducea *et al.* (2020) argues for the subduction of foreland continental lithosphere. Subduction of part of the Moesian Platform might explain the significant Permo-Triassic population, but our data lack the significant peaks that have been observed in the Danubian (e.g. 308, 577 or 806 Ma) and in the Central and Southern Dobrogea (e.g. 612 Ma; Ducea *et al.* 2018; Fig. 9), part of the Western and Eastern Moesian Platform. The majority of models for the genesis of Neogene and Quaternary magmas in the South Apuseni Mountains suggest asthenospheric upwelling and melting of the subcontinental lithospheric mantle and/or lower crust (e.g. Seghedi *et al.* 2022), without any input from the slab, which only acts as a driver of extensional tectonics during its eastwards roll-back. In this instance, a two-step process is

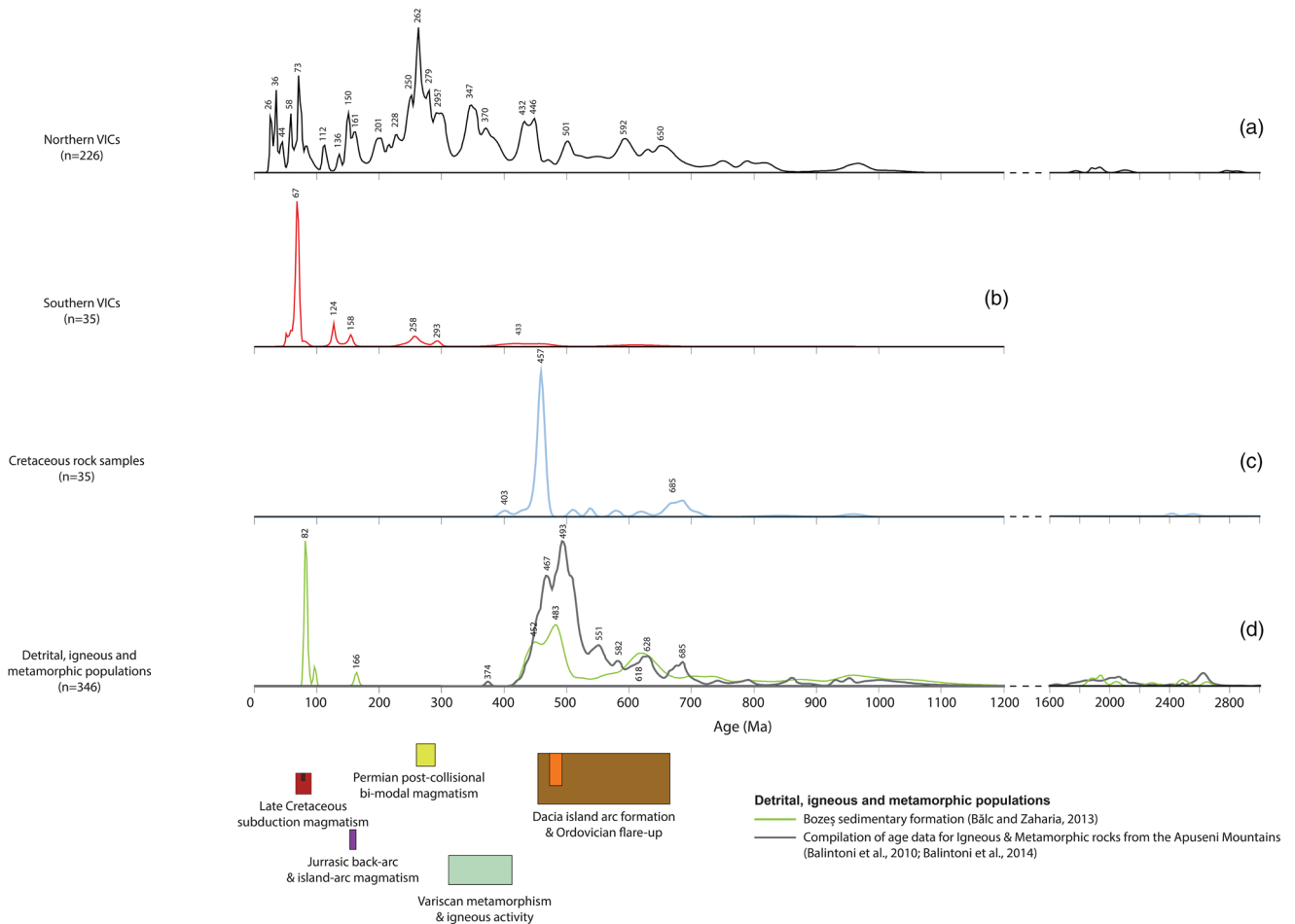


**Fig. 9.** Probability density plots of zircon U–Pb age data for rock samples from (a) the northern volcanic–intrusive complexes (Bucium–Roşia Montană, Zarand, Zlatna, Brad and Baia de Arieş), (b) the southern volcanic–intrusive complexes (Hărţăgani–Săcărâmb, Deva and Uroi), (c) Cretaceous lava flows and (d) the Bozeş sedimentary formation (Bălc and Zaharia 2013) and metamorphic (gneisses, mica schists, metagranites and metadiorites) and igneous rocks (granites; Balintoni *et al.* 2010; Balintoni *et al.* 2014) from the Apuseni Mountains.

required: (1) preconditioning the lower crust and/or the mantle and introducing xenocrystic zircon into the system underneath what will become the South Apuseni Mountains; and (2) melting during Neogene extensional tectonics. An alternative model is proposed by Ducea *et al.* (2020) for the Uroi VIC, a significant bearer of xenocrystic zircon crystals, arguing in favour of a slab-melting origin for the magmas due to their evident adakitic fingerprint.

## Summary

The xenocrystic zircon crystals in the analysed samples from the South Apuseni Mountains capture an intriguing record of crustal complexity at depth (Fig. 9). Our dataset of xenocrystic zircon dates cannot pinpoint one individual source for the observed populations and whether these reflect the source of the magmas or crustal contamination. Nevertheless, this complexity needs to be taken into consideration when discussing the origin and evolution of the Neogene and Quaternary magmatic suites in the South Apuseni Mountains.

## Conclusions

- Based on the newly available U–Pb ages, Neogene magmatism in the South Apuseni Mountains was active between  $13.8 \pm 0.6$  and  $7.3 \pm 0.1$  Ma. During the Quaternary, the Uroi intrusion was emplaced at  $1.5 \pm 0.1$  Ma. Magmatism started in the northern part of the

district in the Bucium–Roşia Montană VIC. This was followed by magmatic activity in the south and west, leading to the formation of most of the Zlatna–Brad, Zarand, Hărţăgani–Săcărâmb and Deva VICs. No east–west preferential migration of magmatic activity has been observed, Zlatna in the east being relatively coeval with Zarand in the west. Magmatism started in the Baia de Arieş VIC at *c.* 9.4 Ma, where it remained active for 2 Myr, ceasing at *c.* 7.3 Ma. The updated timeline for the vertical axis rotations of the South Apuseni Mountains shows that most of the clockwise rotation ( $54.4 \pm 10.7^\circ$ ) took place rapidly between *c.* 14 and 11 Ma, confirming previous studies.

- Inherited zircon crystals are present in all the volcanic–intrusive complexes; however, their frequency differs. Analysed populations in the collected Cretaceous samples match the ages of rock units making up the local crust, with a prominent peak at *c.* 460 Ma. By contrast, a Permo–Triassic population is the most frequent age group detected in the Neogene and Quaternary VICs.
- The ages reported for the local crustal units into which the South Apuseni Mountains Neogene and Quaternary magmas intruded cannot account for the observed xenocrystic zircon crystal populations. Other sources are therefore required. It is unclear how, and in what proportions, these interacted with the analysed Tertiary rocks.

**Acknowledgements** We are grateful to the technical staff at the Geochronology and Tracers Facility, British Geological Survey (Nottingham, UK) for help with zircon separation and the laser ablation inductively coupled plasma mass spectrometry analyses. Simon Tapster and Jonathan Naden publish with the permission of the Executive Director, British Geological Survey (UKRI-NERC).

**Author contributions** VVE: conceptualization (lead), data curation (lead), formal analysis (lead), investigation (lead), validation (lead), visualization (lead), writing – original draft (lead); ST: conceptualization (supporting), data curation (supporting), formal analysis (supporting), funding acquisition (equal), investigation (supporting), methodology (lead), resources (lead), supervision (equal), validation (supporting), visualization (supporting), writing – original draft (supporting), writing – review and editing (lead); DJS: conceptualization (supporting), funding acquisition (equal), investigation (supporting), resources (supporting), supervision (equal), visualization (supporting), writing – original draft (supporting), writing – review and editing (supporting); CP: conceptualization (supporting), investigation (supporting), methodology (supporting), resources (supporting), visualization (supporting), writing – original draft (supporting), writing – review and editing (supporting); ER: conceptualization (supporting), investigation (supporting), resources (supporting), supervision (supporting), writing – review and editing (supporting); JN: conceptualization (supporting), funding acquisition (equal), resources (supporting), supervision (equal), writing – review and editing (supporting); MM: conceptualization (supporting), resources (supporting), writing – review and editing (supporting).

**Funding** This work was funded by a UKRI-NERC CENTA2 UK Doctoral Training Partnership Studentship (Grant NE/S007350/1) and in part by the BGS University Funding Initiative (S344). The isotope analyses were funded by the NERC Isotope Geosciences Facilities Steering Committee (Grant IP-1785-1117). Daniel J. Smith acknowledges support from UKRI-NERC Security of Supply of Minerals Programme (Grant NE/M010848/1).

**Competing interests** The authors declare that they have no known competing financial interests or personal relationships that could have appeared to influence the work reported in this paper.

**Data availability** All data generated or analysed during this study are included in this published article (and if present, its [supplementary information files](#)).

## References

- Balázs, A., Maţenco, L., Magyar, I., Horváth, F. and Cloetingh, S. 2016. The link between tectonics and sedimentation in back-arc basins: new genetic constraints from the analysis of the Pannonian Basin. *Tectonics*, **35**, 1526–1559, <https://doi.org/10.1002/2015TC004109>
- Bălc, R. and Zaharia, L. 2013. Sedimentary deposition of Bozeş Formation (Apuseni Mts., Romania)–detrital zircon dating and micropaleontological ages. *Studia Universitatis Babeş-Bolyai Geologia*, **58**, 29–40, <https://doi.org/10.5038/1937-8602.58.2.4>
- Balica, C., Ducea, M., Costin, G. and Balintoni, I. 2008. Timing of metamorphism in the Baia de Aries sequence (Apuseni Mts, Romania). Paper presented at the 33rd International Geological Congress, 6–14 August, Oslo, Norway.
- Balintoni, I. and Balica, C. 2012. Avalonian, Ganderian and East Cadomian terranes in South Carpathians, Romania, and Pan-African events recorded in their basement. *Mineralogy and Petrology*, **107**, 709–725, <https://doi.org/10.1007/s00710-012-0206-x>
- Balintoni, I. and Balica, C. 2013. Carpathian peri-Gondwanan terranes in the East Carpathians (Romania): a testimony of an Ordovician, North-African orogeny. *Gondwana Research*, **23**, 1053–1070, <https://doi.org/10.1016/j.gr.2012.07.013>
- Balintoni, I.C., Balica, C., Zaharia, L., Cliveti, M., Chen, F., Hann, H.P. and Li, L.Q. 2007. The age of the Variscan suture in the Apuseni Mountains, Romania, as revealed by LA-ICP-MS zircon dating. *AGU Fall Meeting*, 10–14 December 2007, Abstracts, V13A–1139
- Balintoni, I., Balica, C., Cliveti, M., Li, L.-Q., Hann, H., Chen, F. and Schuller, V. 2009. The emplacement age of the Muntele Mare Variscan granite (Apuseni Mountains, Romania). *Geologica Carpathica*, **60**, 495–504, <https://doi.org/10.2478/v10096-009-0036-x>
- Balintoni, I., Balica, C. et al. 2010. Late Cambrian–Ordovician northeastern Gondwanan terranes in the basement of the Apuseni Mountains, Romania. *Journal of the Geological Society, London*, **167**, 1131–1145, <https://doi.org/10.1144/0016-76492009-156>
- Balintoni, I., Balica, C., Ducea, M.N. and Hann, H.-P. 2014. Peri-Gondwanan terranes in the Romanian Carpathians: a review of their spatial distribution, origin, provenance, and evolution. *Geoscience Frontiers*, **30**, 395–411, <https://doi.org/10.1016/j.gsf.2013.09.002>
- Balla, Z. 1987. Tertiary palaeomagnetic data for the Carpatho-Pannonian region in the light of Miocene rotation kinematics. *Tectonophysics*, **139**, 67–98, [https://doi.org/10.1016/0040-1951\(87\)90198-3](https://doi.org/10.1016/0040-1951(87)90198-3)
- Bortolotti, V., Marroni, M., Nicolae, I., Pandolfi, L., Principi, G. and Saccani, E. 2002. Geodynamic implications of Jurassic ophiolites associated with island-arc volcanics, South Apuseni Mountains, Western Romania. *International Geology Review*, **44**, 938–955, <https://doi.org/10.2747/0020-6814.44.10.938>
- Brek, M., Gaynor, S.P. et al. 2021. Karst bauxite formation during Miocene climatic optimum (central Dalmatia, Croatia): mineralogical, compositional and geochronological perspectives. *International Journal of Earth Sciences*, **110**, 2899–2922, <https://doi.org/10.1007/s00531-021-02091-z>
- Burchfiel, B. and Royden, L. 1982. Carpathian foreland fold and thrust belt and its relation to Pannonian and other basins. *AAPG Bulletin*, **66**, 1179–1195.
- Cherniak, D. and Watson, E. 2001. Pb diffusion in zircon. *Chemical Geology*, **172**, 5–24, [https://doi.org/10.1016/S0009-2541\(00\)00233-3](https://doi.org/10.1016/S0009-2541(00)00233-3)
- Debiche, M. and Watson, G. 1995. Confidence limits and bias correction for estimating angles between directions with applications to paleomagnetism. *Journal of Geophysical Research: Solid Earth*, **100**, 24405–24429, <https://doi.org/10.1029/92JB01318>
- Downes, H., Vaselli, O. et al. 1995. Geochemistry of late Cretaceous–early Tertiary magmatism in Poiana Ruscă (Romania). *Acta Vulcanologica*, **7**, 209–217.
- Drăguşanu, C. and Tanaka, T. 1999. 1.57-Ga Magmatism in the south Carpathians: implications for the pre-alpine basement and evolution of the mantle under the European continent. *Journal of Geology*, **107**, 237–248, <https://doi.org/10.1086/314344>
- Ducea, M.N., Giosan, L. et al. 2018. U–Pb detrital zircon geochronology of the lower Danube and its tributaries: implications for the geology of the Carpathians. *Geochemistry, Geophysics, Geosystems*, **19**, 3208–3223, <https://doi.org/10.1029/2018gc007659>
- Ducea, M.N., Barla, A., Stoica, A.M., Panaiotu, C. and Petrescu, L. 2020. Temporal–geochemical evolution of the Persani volcanic field, Eastern Transylvanian Basin (Romania): implications for slab rollback beneath the SE Carpathians. *Tectonics*, **39**, e2019TC005802, <https://doi.org/10.1029/2019tc005802>
- Fedele, L., Seghedi, I., Chung, S.-L., Laiena, F., Lin, T.-H., Morra, V. and Lustrino, M. 2016. Post-collisional magmatism in the Late Miocene Rodna–Bărgău district (East Carpathians, Romania): geochemical constraints and petrogenetic models. *Lithos*, **266–267**, 367–382, <https://doi.org/10.1016/j.lithos.2016.10.015>
- Fisher, R.A. 1953. Dispersion on a sphere. *Proceedings of the Royal Society of London. Series A. Mathematical and Physical Sciences*, **217**, 295–305, <https://doi.org/10.1098/rspa.1953.0064>
- Gallhofer, D., Quadt, A.V., Peytcheva, I., Schmid, S.M. and Heinrich, C.A. 2015. Tectonic, magmatic, and metallogenic evolution of the Late Cretaceous arc in the Carpathian–Balkan Orogen. *Tectonics*, **34**, 1813–1836, <https://doi.org/10.1002/2015tc003834>
- Gallhofer, D., von Quadt, A., Schmid, S.M., Guillong, M., Peytcheva, I. and Seghedi, I. 2017. Magmatic and tectonic history of Jurassic ophiolites and associated granitoids from the South Apuseni Mountains (Romania). *Swiss Journal of Geosciences*, **110**, 699–719, <https://doi.org/10.1007/s00015-016-0231-6>
- Ghiţulescu, T.P. and Socolescu, M. 1941. Etude géologique et minière des Monts Métallifères (Quadrilatère aurifère et régions environnantes). *Annuaire de l'Institut Géologique Roumain*, **21**, 181–463.
- Harangi, S. 2001. Neogene to Quaternary volcanism of the Carpathian–Pannonian Region – a review. *Acta Geologica Hungarica*, **44**, 223–258.
- Harangi, S., Wilson, M. and Tonarini, S. 1995. Petrogenesis of Neogene potassic volcanic rocks in the Pannonian Basin. *Acta Vulcanologica*, **7**, 125–134.
- Harris, C., Pettko, T., Heinrich, C.A., Rosu, E., Woodland, S. and Fry, B. 2013. Tethyan mantle metasomatism creates subduction geochemical signatures in non-arc Cu–Au–Te mineralizing magmas, Apuseni Mountains (Romania). *Earth and Planetary Science Letters*, **366**, 122–136, <https://doi.org/10.1016/j.epsl.2013.01.035>
- Hoek, V., Ionescu, C., Balintoni, I. and Koller, F. 2009. The Eastern Carpathians ‘ophiolites’ (Romania): remnants of a Triassic ocean. *Lithos*, **108**, 151–171, <https://doi.org/10.1016/j.lithos.2008.08.001>
- Holder, D.S. 2016. *Geological and Geochemical Controls for Epithermal Au–Ag–Te (Pb–Zn) Mineralisation at Coranda-Hondol and the Brad-Săcărâmb Basin Mineral District of Western Romania*. PhD thesis, Kingston University London.
- Hora, J.M., Singer, B.S., Jicha, B.R., Beard, B.L., Johnson, C.M., de Silva, S. and Salisbury, M. 2010. Volcanic biotite–sanidine  $^{40}\text{Ar}/^{39}\text{Ar}$  age discordances reflect Ar partitioning and pre-eruption closure in biotite. *Geology*, **38**, 923–926, <https://doi.org/10.1130/g31064.1>
- Ianovici, V., Borcos, M., Bleahu, M., Patrulea, D., Lupu, M., Dimitrescu, R. and Savu, H. 1976. *Geologia Muntilor Apuseni*. Ed. Academiei, Bucharest.
- Ismail-Zadeh, A., Matenco, L., Radulian, M., Cloetingh, S. and Panza, G. 2012. Geodynamics and intermediate-depth seismicity in Vrancea (the south-eastern Carpathians): current state-of-the-art. *Tectonophysics*, **530–531**, 50–79, <https://doi.org/10.1016/j.tecto.2012.01.016>
- Karáton, D., Wulf, S. et al. 2016. The latest explosive eruptions of Ciomadul (Csomád) volcano, East Carpathians – a tephrostratigraphic approach for the 51–29 ka BP time interval. *Journal of Volcanology and Geothermal Research*, **319**, 29–51, <https://doi.org/10.1016/j.jvolgeores.2016.03.005>



- Porphyry Prospect, Solomon Islands. *Earth and Planetary Science Letters*, **442**, 206–217, <https://doi.org/10.1016/j.epsl.2016.02.046>
- Vander Auwera, J., Berza, T., Gesels, J. and Dupont, A. 2016. The Late Cretaceous igneous rocks of Romania (Apuseni Mountains and Banat): the possible role of amphibole versus plagioclase deep fractionation in two different crustal terranes. *International Journal of Earth Sciences*, **105**, 819–847, <https://doi.org/10.1007/s00531-015-1210-2>
- van Hinsbergen, D.J.J., Torsvik, T.H. et al. 2020. Orogenic architecture of the Mediterranean region and kinematic reconstruction of its tectonic evolution since the Triassic. *Gondwana Research*, **81**, 79–229, <https://doi.org/10.1016/j.gr.2019.07.009>
- Vermeesch, P. 2012. On the visualisation of detrital age distributions. *Chemical Geology*, **312**, 190–194, <https://doi.org/10.1016/j.chemgeo.2012.04.021>
- Vlasceanu, M., Ducea, M.N., Luffi, P., Barla, A. and Seghedi, I. 2021. Carpathian–Pannonian magmatism database. *Geochemistry, Geophysics, Geosystems*, **22**, e2021GC009970, <https://doi.org/10.1029/2021GC009970>
- von Quadt, A., Moritz, R., Peytcheva, I. and Heinrich, C.A. 2005. 3: Geochronology and geodynamics of Late Cretaceous magmatism and Cu–Au mineralization in the Panagyurishte region of the Apuseni–Banat–Timok–Srednogie belt, Bulgaria. *Ore Geology Reviews*, **27**, 95–126, <https://doi.org/10.1016/j.oregeorev.2005.07.024>
- Wendt, I. and Carl, C. 1991. The statistical distribution of the mean squared weighted deviation. *Chemical Geology: Isotope Geoscience Section*, **86**, 275–285, [https://doi.org/10.1016/0168-9622\(91\)90010-T](https://doi.org/10.1016/0168-9622(91)90010-T)
- Zaharia, L., Gärtner, A., Hofmann, M. and Linnemann, U. 2018. U–Pb detrital zircon ages of the Upper Cretaceous Groși Unit (Apuseni Mts, Romania)—constraining the potential sediment sources. In: Neubauer, F., Brendel, U. and Friedl, G. (eds) *Advances of Geology in Southeast European Mountain Belts, XXI International Congress of the Carpathian Balkan Geological Association (CBGA), 10–13 September 2018, Salzburg, Austria*. Bulgarian Academy of Sciences and the Geological Institute “Strashimir Dimitrov”, Sofia.